

# DriveMLLM: A Benchmark for Spatial Understanding with Multimodal Large Language Models in Autonomous Driving

Xianda Guo<sup>1,\*</sup>, Ruijun Zhang<sup>2,3,\*</sup>, Yiqun Duan<sup>4,\*</sup>, Yuhang He<sup>5</sup>,  
Chenming Zhang<sup>6,3</sup>, Shuai Liu<sup>7</sup>, Long Chen<sup>2,3,6,†</sup>

<sup>1</sup> School of Computer Science, Wuhan University

<sup>2</sup> Institute of Automation, Chinese Academy of Sciences <sup>3</sup> Waytous

<sup>4</sup> HAI Centre, AAIL, School of Computer Science, University of Technology Sydney

<sup>5</sup> Department of Computer Science, University of Oxford. UK. <sup>7</sup> TikTok

<sup>6</sup> Institute of Artificial Intelligence and Robotics, Xi'an Jiaotong University

## Abstract

Autonomous driving requires a comprehensive understanding of 3D environments to facilitate high-level tasks such as motion prediction, planning, and mapping. In this paper, we introduce DriveMLLM, a benchmark specifically designed to evaluate the spatial understanding capabilities of multimodal large language models (MLLMs) in autonomous driving. DriveMLLM includes 880 front-facing camera images and introduces both absolute and relative spatial reasoning tasks, accompanied by linguistically diverse natural language questions. To measure MLLMs' performance, we propose novel evaluation metrics focusing on spatial understanding. We evaluate several state-of-the-art MLLMs on DriveMLLM, and our results reveal the limitations of current models in understanding complex spatial relationships in driving contexts. We believe these findings underscore the need for more advanced MLLM-based spatial reasoning methods and highlight the potential for DriveMLLM to drive further research in autonomous driving. Code will be available at <https://github.com/XiandaGuo/Drive-MLLM>.

## 1. Introduction

One of the primary tasks for vision-based autonomous driving system is to achieve holistic 3D scene understanding from visual images or videos [9], which essentially serve fundamental information for further high-level tasks such as motion prediction [29, 32, 52, 57, 77], planning [8, 45, 62] and map construction [19, 73]. While we have witnessed huge progress in per-object centered recognition tasks with

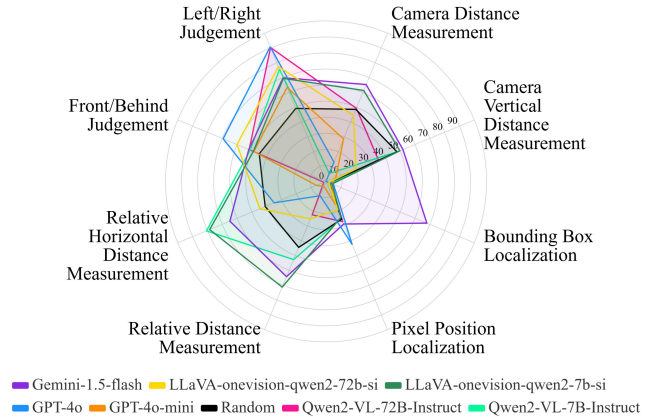


Figure 1. Visualization of different MLLMs' performance measured by success-rate-weighted average accuracy across each spatial understanding capability.

the assistance of various large scale dataset [20, 30, 56], including detection [34, 35], tracking [24, 38], optical flow estimation [22, 55] and semantic segmentation [17, 36], the inter-object spatial relation reasoning from RGB images in autonomous driving has been ignored even though its vital importance in achieving fully holistic 3D scene understanding.

In computer vision, within image spatial relation reasoning has been thoroughly studied [65] with the assistance of large-scale visual genome dataset [40]. However, prior works mainly focus on simple relations. For example, the left/right and top/bottom are relative position relations. These simple relations are far from fully representing the potential complex spatial relations that are present in the 3D scene. The emergence of large language models (LLM) [58, 70] in recent years has largely unlocked the potential to address various high-level vision

\*These authors contributed equally to this work.

†Corresponding authors: long.chen@ia.ac.cn

tasks [1, 5, 15, 16, 21, 23, 48, 49, 53, 72].

Although the aforementioned huge advancement and dramatic progress we have achieved in various multimodal large language models (MLLM) based tasks, the multimodal large language models based spatial understanding in autonomous driving still awaits to be tackled. As discussed in the last two paragraphs, pre-LLM era spatial understanding unanimously focuses on per-object recognition tasks. However, inter-object spatial understanding is essential to achieve high-level and holistic autonomous driving scene understanding. Benefiting from the huge potential and powerfulness of LLM and the progress we have witnessed in recent years, we propose to tackle high-level, inter-object spatial understanding by leveraging MLLMs. In this paper, we propose a large-scale benchmark, dubbed DriveMLLM, tailored for autonomous driving spatial understanding tasks with MLLMs.

We meticulously curate DriveMLLM from the nuScenes [11] dataset, a large-scale autonomous driving dataset. As the nuScenes [11] dataset contains images from six cameras covering a full 360° field of view, it serves as an ideal data source for constructing DriveMLLM benchmark and ensures the curated benchmark is grounded in realistic driving scenarios. Specifically, we focused on the images from the front-facing camera in the validation split of the nuScenes [11] dataset. We have curated 880 images with objects of interest that have a clear appearance. For the spatial relations, we focus on both absolute spatial reasoning and relative positional relationship reasoning. We further construct linguistically diverse and contextually similar natural language questions (as shown in Figure 2) and propose new corresponding evaluation metrics to evaluate the spatial understanding capabilities of various MLLMs. We comprehensively evaluate DriveMLLM on various MLLM models, as shown in Figure 1. In summary, we make three main contributions to this work:

1. We propose a large benchmark, called DriveMLLM, for spatial understanding in autonomous driving with multimodal large language models (MLLMs), a research topic that has not yet been discussed of vital importance.
2. We base DriveMLLM on nuScenes [11] dataset. It comprises 880 images and diverse natural language-based questions. DriveMLLM introduces both absolute and relative spatial relation reasoning tasks, which is essential for achieving holistic autonomous driving scene understanding.
3. We verify DriveMLLM on various MLLM models, showing the incapability of most MLLM models in autonomous driving spatial understanding. In turn, it exhibits the importance and huge potential of our introduced DriveMLLM benchmark for facilitating further research.

## 2. Related Work

### 2.1. Multimodal Large Language Models (MLLM)

Benefiting from the huge success in large language models (LLMs) [10, 58, 59] in recent years, a new research venue has been focusing on extending natural language-based large models (especially the GPT family LLM) to multimodal large language models (MLLM) [1, 25, 43, 44, 63, 69]. Among all of them, encompassing vision into language has made dramatic progress and various vision language models (VLM) have been developed [6, 7, 43, 44, 47, 48] for various crossmodal tasks such as visual question answer (VQA) [3, 31] and crossmodal reasoning [28, 37, 68, 76], owing to the availability of various large image-text datasets [12, 39, 46, 66]. Typical VLM models include BLIP family [43, 44], LLaVA family [47, 48] and Qwen-VL family [4, 6, 71]. They either innovate in network architecture [18, 43, 44, 61] or adopt novel training strategy [6, 78]. For example, regarding the network architecture innovation, Qwen-VL [6] and MiniGPT-4 [78] employ ViT [2] like network as visual encoder, LLaVA [61] instead employs CLIP ViT-L/14 [64] for visual encoding and InternVL [18] uses InternViT-6B for visual encoding. Regarding the training strategy, Qwen-VL [6] employs a three-stage strategy: first pre-train on massive image-text pairs, then multi-task pre-train over seven major tasks, and finally fine-tune with instruction on over 350,000 dialogues. MiniGPT-4 [78] adopts a two-stage training strategy by first pre-training on composite dataset including Conceptual Captions [13], LAION [67] and SBU [60] and then fine-tuning on high-quality image description dataset.

### 2.2. Multimodal Large Language Models Benchmark

In the pre-LLM era, most public multimodal vision-language datasets are single-task based and lack the ability to holistically evaluate multimodal LLMs much broad and general reasoning capability. For example, those typical datasets simply focus on single-task including image caption [46], VQA [3, 31] and optical character recognition (OCR) [51]. In the LLM era, more powerful and comprehensive multimodal datasets have been curated and released for various holistic and multi-task evaluation purposes, hugely scaling up the potential and possibility for designing various powerful multimodal large language model frameworks. Among all of them, MME [26] is one of the earliest benchmarks for multimodal *Yes/No* question, visual perception, and language reasoning tasks. MM-Bench [50] extends to encompass much more diverse subjects and a more robust circular evaluation setting. Seed-Bench [41, 42] introduces much more diverse input sources, such as multiple-image inputs and video. MM-Vet [74] integrates six sub-features from previous datasets, resulting

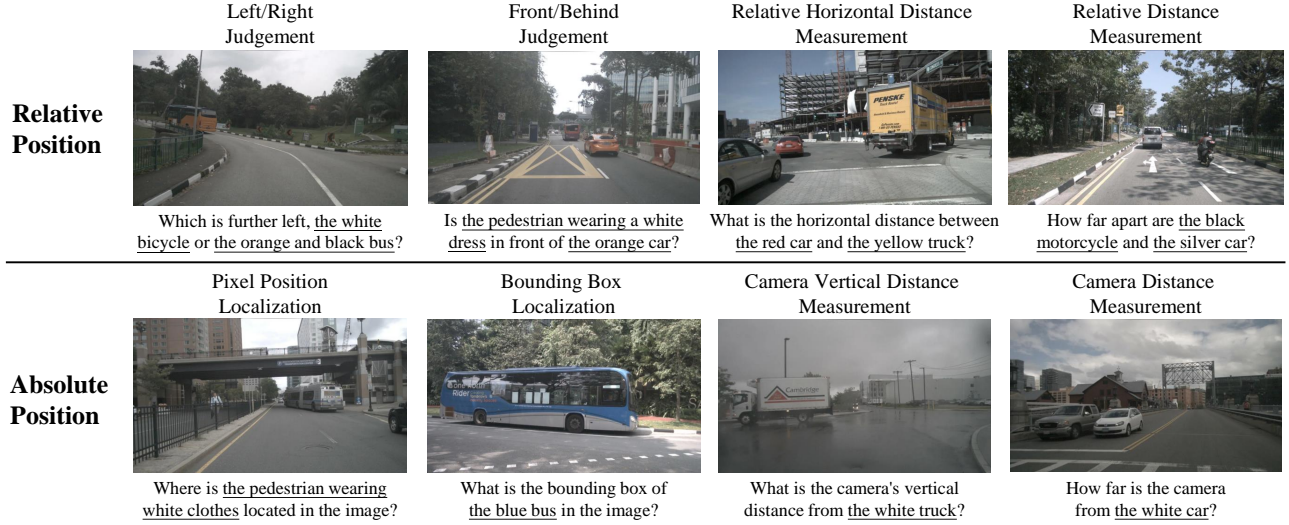


Figure 2. Illustration of the constructed questions for different spatial understanding capacities.

in multi-task reasoning capabilities like OCR, recognition-focused questions, and math. Other than MME [26], MM-Bench [50], Seed-Bench [41, 42] and MM-Vet [74] that mostly focus on recognition, more recent datasets focus on more generalized artificial intelligence capability. For example, MMMU [75] has collected large-scale domain-knowledge-required questions to push the boundary of general artificial intelligence. HallusionBench [33] datasets aims to the language hallucination and visual illusion phenomena. MathVista [54] instead exclusively focuses on math-centered visual questions based on images such as charts, tables, and diagrams. BLINK [27] datasets introduce human-level perception ability to achieve holistic visual perception. Mega-Bench [14] scales up the multimodal evaluation to over 500 real-world tasks. Although those various benchmarks, the corresponding benchmark focusing on spatial understanding in autonomous driving is missing and we tend to fill in the gap in this work.

### 3. DriveMLLM Benchmark

Recent advancements have seen MLLMs being directly employed for autonomous driving and embodied intelligence, which heavily depend on sophisticated spatial perception and reasoning. However, these works lack a detailed investigation into the spatial reasoning abilities of MLLMs to convince how reliable current MLLMs are on spatial information. In this section, we introduce how we construct the DriveMLLM Benchmark as below, where section 3.1 provides detailed descriptions of the data source we build this benchmark. Section 3.2 provides detailed label construction processes and filtering processes.

#### 3.1. Data Source

We constructed our benchmark using data from the nuScenes [11] dataset, which is a large-scale public dataset specifically designed for autonomous driving research. It collects rich sensor data, including images from six cameras covering a full 360° field of view, along with LiDAR, radar, and GPS/IMU data. The dataset was captured in the urban environments of Boston and Singapore, featuring a diverse range of traffic conditions, weather scenarios, and times of day. This diversity ensures that the models are tested on a wide array of real-world driving situations, enhancing the robustness of the evaluation.

For our benchmark, we focused on the images from the front-facing camera in the validation split of the nuScenes [11] dataset. This subset includes complex scenes with dynamic and static objects such as vehicles and pedestrians. The images are high-resolution and come with comprehensive annotations, making them ideal for tasks requiring detailed spatial understanding.

#### 3.2. Data Filtering

We curated a dataset of 880 images through a meticulous data filtering and refinement process. This multi-step filtering ensured that each image supported unambiguous spatial reasoning. The data filtering process comprises four main steps detailed below.

**1. Initial Image Selection from nuScenes [11]** We began by extracting images from the front-facing camera in the validation set of the nuScenes [11] dataset. This initial selection yielded 6,019 images containing objects of interest, such as vehicles and pedestrians.

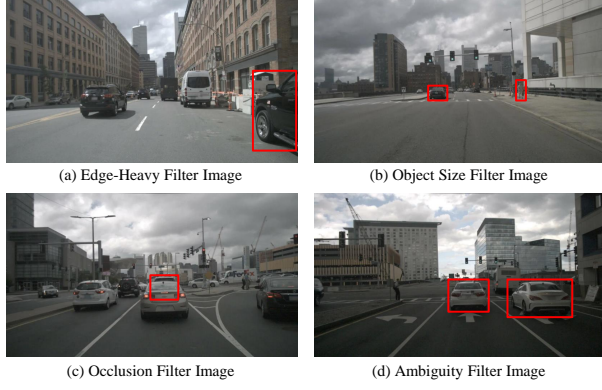


Figure 3. Data filtering process on nuScenes dataset.

**2. Filtering for Validity and Relevance** To ensure suitability for spatial reasoning evaluation, we applied rigorous filtering criteria:

- **Edge-Heavy Filter:** We excluded objects whose centers do not appear within the frame, as they are too marginal for effective evaluation (see Figure 3(a)). This preserves the integrity of the objects being analyzed.
- **Object Size Filter:** Pedestrians with bounding box widths smaller than 40 pixels and vehicles with bounding box areas less than 2,000 pixels were excluded, as they are too small for reliable assessment (see Figure 3(b)). This ensures adequate visibility and discernibility of the objects.
- **Occlusion Filter:** We removed images exhibiting significant occlusion, defined as overlapping objects where the intersection area exceeds 30% of the smaller bounding box (see Figure 3(c)). This guarantees that each object remains sufficiently visible and not excessively obscured.
- **Ambiguity Filter:** To mitigate ambiguity, we excluded images containing multiple instances of the same object type (e.g., two pedestrians or several vehicles), as illustrated in Figure 3(d). This ensures that each image presents a distinct, unambiguous object for evaluation.

After applying these filters, we retained 2,734 images with clear and visible objects.

**3. Manual Review and Final Selection** Despite the automated filtering, some images still exhibited issues such as ambiguities, occlusions, or unmarked objects (e.g., guard posts partially obstructing vehicles). We conducted a manual review to further refine the dataset, selecting 880 images that featured single, unambiguous, and clearly visible objects with discernible attributes.

**4. Generating Natural Language Descriptions** To address the absence of natural language descriptions in the nuScenes [11] dataset—essential for evaluating multimodal

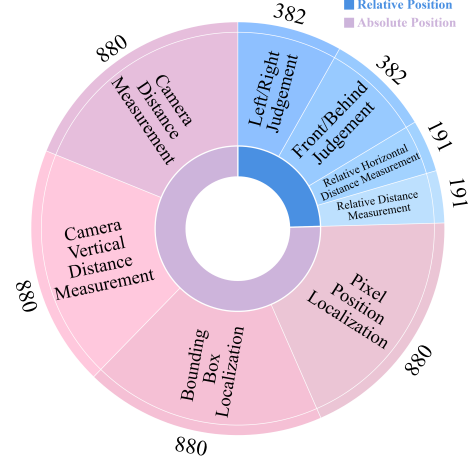


Figure 4. Distribution of question types among spatial understanding tasks in the DriveMLLM benchmark.

LLMs—we generated standardized descriptive text for each object using a 13B-parameter InstructBLIP model to minimize bias toward specific LLM conventions. Pedestrians were identified by clothing (e.g., “the pedestrian wearing a red shirt”), and vehicles by color (e.g., “the red truck”), ensuring consistency across descriptions and supporting robust evaluation of model spatial understanding.

### 3.3. Benchmark Construction

To evaluate the spatial understanding capabilities of MLLMs in the autonomous driving scenario and answer the questions proposed above, designed a comprehensive benchmark focusing on two key aspects: **absolute spatial reasoning** and **relative positional relationships**.

**Absolute Spatial Reasoning Tasks** These tasks evaluate the model’s ability to determine precise spatial information about objects within an image, requiring an understanding of pixel-level details. To provide an intuitive understanding, we visualize these tasks and present them in Figure 2.

1. **Object Localization Coordinates:** The model must identify and provide the exact coordinates  $[x, y]$  of a specified object in the image. This task tests the ability to pinpoint objects accurately within the image plane.  
*Question:* Where is {} located in the image?
2. **Object Bounding Box Determination:** This task involves calculating the bounding box coordinates  $[min\_x, min\_y, max\_x, max\_y]$  of a specific object. It assesses the model’s capability to delineate the spatial extent of objects.  
*Question:* What is the bounding box of {} in the image?
3. **Camera-to-Object Distance Estimation:** The model computes the Euclidean distance from the camera to a



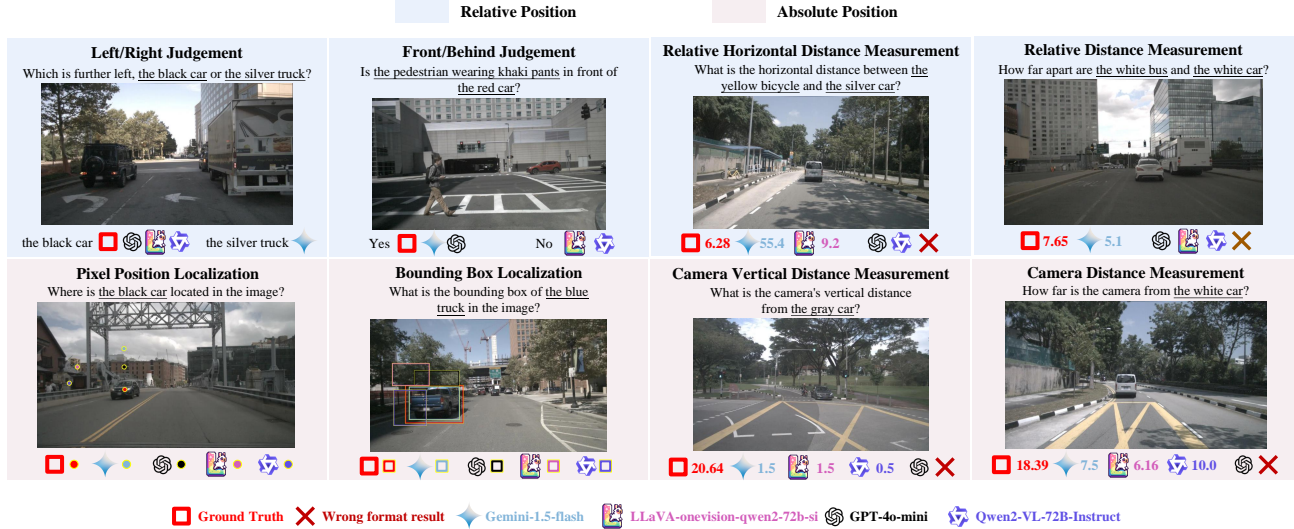


Figure 5. Qualitative visualization on the generated answer to each spatial question.

specified object using inferred spatial information. This evaluates the model’s depth perception and distance estimation skills.

*Question:* How far is the camera from {}?

4. **Vertical Distance Calculation:** The task requires calculating the vertical distance between the camera and an object based on the object’s  $z$ -coordinate. This tests the model’s understanding of vertical spatial relationships.  
*Question:* What is the camera’s vertical distance from {}?

**Relative Positional Relationship Tasks** These tasks assess the model’s ability to understand and compare the spatial relationships between multiple objects within a scene. To further illustrate these concepts, we provide visual examples in Figure 2.

5. **Leftmost/Rightmost Object Identification:** The model determines which of two specified objects is positioned further to the left/right in the image, testing lateral spatial reasoning based on inferred  $x$ -coordinates.  
*Question:* Which is further left/right, {} or {}?
6. **Front/Back Position Determination:** The model assesses whether one object is in front of another or whether one object is behind another based on depth cues, evaluating understanding of  $z$ -coordinate relationships.  
*Question:* Is {} in front of/behind {}?
7. **Inter-Object Distance Measurement:** This task involves calculating the Euclidean distance between two objects in three-dimensional space, assessing comprehensive spatial reasoning.  
*Question:* How far apart are {} and {}?

#### 8. Horizontal Distance Calculation Between Objects:

The model calculates the horizontal distance between two objects, defined as the absolute difference in their  $x$ -coordinates, testing precise lateral distance estimation.

*Question:* What is the horizontal distance between {} and {}?

**Task Format and Evaluation Protocol** For each task, models are provided with an image and a corresponding question formatted as specified. To ensure consistency and facilitate automated evaluation, models must output their answers within designated markers.

## 4. Experiment

### 4.1. Experimental Setup

To evaluate the spatial reasoning capabilities of MLLMs within the autonomous driving context, we conducted experiments using the DriveMLLM benchmark described earlier. We selected a diverse set of state-of-the-art MLLMs for evaluation, including GPT-4o, GPT-4o-mini, LLaVA one vision models (LLaVA-ov-7b and LLaVA-ov-72b), Qwen2-VL models (qwen2-vl-7b and qwen2-vl-72b), and Gemini-1.5-Flash. These models vary in size and training data, providing a comprehensive assessment across different architectures.

We tested each model under three experimental settings: zero-shot, one-shot, and five-shot learning. In the zero-shot setting, models were evaluated without any task-specific examples. The one-shot and five-shot settings provided the models with one and five exemplars to assess their ability to leverage few-shot learning for improved performance.

All models were prompted with the standardized questions and required to produce outputs adhering strictly to the specified format, ensuring fairness and consistency in evaluation.

## 4.2. Metrics

To quantitatively evaluate the performance of the models on the DriveMLLM benchmark, we define a set of metrics that measure the accuracy and efficiency of the models across various tasks. Let  $N$  denote the total number of samples in the test set. For each sample  $i$ , the model produces a prediction, which is compared against the ground truth to compute an individual accuracy score  $acc_i$  and an efficiency indicator  $eff_i$ . The overall metrics are then aggregated over all samples.

### 4.2.1 Accuracy Metrics

The accuracy metrics quantify the correctness of the model’s predictions for different types of tasks. The individual accuracy  $acc_i$  for each sample  $i$  is defined based on the task type as follows:

**Binary Classification Accuracy (Tasks L/R, F/B)** For binary classification tasks, such as Left/Right (L/R) judgment and Front/Behind (F/B) judgment, the individual accuracy  $acc_i$  is defined as:

$$acc_i = \begin{cases} 1, & \text{if } p_i = y_i \\ 0, & \text{if } p_i \neq y_i \end{cases} \quad (1)$$

where: -  $p_i$  is the model’s predicted label for sample  $i$ . -  $y_i$  is the ground truth label for sample  $i$ .

The overall accuracy  $acc$  is calculated as the mean of the individual accuracies:

### Distance-Based Accuracy (Tasks RHD, RD, CVD, CD)

For tasks involving distance measurements—Relative Horizontal Distance (RHD), Relative Distance (RD), Camera Vertical Distance (CVD), and Camera Distance (CD)—the individual accuracy  $acc_i$  is computed using:

$$acc_i = \frac{1}{1 + \alpha_d \|d_i - d_i^{gt}\|_1} \quad (2)$$

where: -  $d_i$  is the model’s predicted distance for sample  $i$ . -  $d_i^{gt}$  is the ground truth distance for sample  $i$ . -  $\alpha_d$  is a scaling factor controlling the penalty for deviation, set to  $\alpha_d = 0.05$ .

**Position Localization Accuracy (Task PPos)** For the pixel position localization task, the individual accuracy  $acc_i$  is based on the Euclidean distance error between the predicted and ground truth coordinates:

$$acc_i = \frac{1}{1 + \alpha_p \|\mathbf{x}_i - \mathbf{x}_i^{gt}\|_2} \quad (3)$$

where: -  $\mathbf{x}_i = (x_i, y_i)$  are the model’s predicted coordinates for sample  $i$ . -  $\mathbf{x}_i^{gt} = (x_i^{gt}, y_i^{gt})$  are the ground truth coordinates for sample  $i$ . -  $\alpha_p$  is a scaling factor, set to  $\alpha_p = 0.005$ .

**Bounding Box Accuracy (Task BBox)** For the bounding box localization task, accuracy is measured using the Intersection over Union (IoU) between the predicted and ground truth bounding boxes:

$$acc_i = \text{IoU}(B_i, B_i^{gt}) = \frac{|B_i \cap B_i^{gt}|}{|B_i \cup B_i^{gt}|} \quad (4)$$

where: -  $B_i$  is the model’s predicted bounding box for sample  $i$ . -  $B_i^{gt}$  is the ground truth bounding box for sample  $i$ . -  $|\cdot|$  denotes the area of the bounding box.

**Aggregate Accuracy Score** The Aggregate Accuracy Score (AccS) combines the individual accuracies across all tasks and samples:

$$acc = \frac{1}{N} \sum_{i=1}^N acc_i \quad \text{AccS} = \frac{1}{8} \sum_{j=1}^8 acc_j \quad (5)$$

### 4.2.2 Efficiency Metrics

Efficiency metrics assess the model’s compliance with the required output format, which is crucial for automated evaluation. For each sample  $i$ , we define the efficiency indicator  $eff_i$  as:

$$eff_i = \begin{cases} 1, & \text{correctly formatted} \\ 0, & \text{otherwise} \end{cases} \quad (6)$$

The Efficiency Score (EffS) is calculated as:

$$eff = \frac{1}{N} \sum_{i=1}^N eff_i \quad \text{EffS} = \frac{1}{8} \sum_{j=1}^8 eff_j \quad (7)$$

### 4.2.3 Final Score

The Final Score integrates both accuracy and efficiency to provide a comprehensive evaluation of the model’s performance:

$$\text{score}_j = acc_j \times eff_j \quad \text{Score} = \frac{1}{8} \sum_{j=1}^8 \text{score}_j \quad (8)$$

N-shot	Model	Relative Position				Absolute Position					
		L/R	F/B	RHD	RD	PPos	BBox	CVD	CD	AccS	Score
	Random	49.22	45.03	41.03	44.52	25.46	2.05	47.93	48.59	37.98	37.98
Zero-shot	GPT-4o	<b>91.72</b>	<b>67.60</b>	9.58	14.69	<b>40.90</b>	<u>4.07</u>	<u>46.11</u>	<b>70.65</b>	<u>43.16</u>	<u>25.63</u>
	GPT-4o-mini	67.67	50.13	<u>70.44</u>	0.00	29.28	3.78	0.00	46.40	33.46	16.68
	LLaVA-ov-7b	73.35	48.70	<b>71.44</b>	0.00	20.00	0.54	0.00	0.00	26.75	22.29
	LLaVA-ov-72b	85.42	49.48	13.76	<u>45.27</u>	16.46	0.00	42.97	27.09	35.06	21.10
	Qwen2-vl-7b	73.72	51.44	26.27	24.14	22.76	1.02	22.17	31.48	31.62	21.17
	Qwen2-vl-72b	<u>89.80</u>	51.30	0.00	0.00	<u>30.59</u>	1.20	0.00	0.00	21.61	20.11
	Gemini-1.5-flash	70.92	<u>52.88</u>	24.16	<b>69.60</b>	29.43	<b>68.46</b>	<b>65.17</b>	<u>67.92</u>	<b>56.07</b>	<b>54.03</b>
One-shot	GPT-4o	<b>91.08</b>	<b>69.37</b>	36.51	71.17	<b>42.44</b>	<u>5.10</u>	0.00	<u>63.88</u>	47.44	33.17
	GPT-4o-mini	66.00	48.95	<b>83.02</b>	58.47	25.71	3.97	<u>52.73</u>	55.23	49.26	22.13
	LLaVA-ov-7b	71.30	48.95	78.46	71.34	24.29	4.16	49.88	61.91	51.29	<u>50.97</u>
	LLaVA-ov-72b	79.12	<u>62.97</u>	49.26	68.04	28.57	2.20	<b>53.12</b>	60.90	50.52	36.66
	Qwen2-vl-7b	77.34	51.05	<u>80.61</u>	<u>73.02</u>	25.45	2.88	49.78	53.39	<u>51.69</u>	42.79
	Qwen2-vl-72b	<u>90.31</u>	51.84	48.33	<b>75.63</b>	27.15	3.86	49.44	60.87	50.93	35.22
	Gemini-1.5-flash	70.45	52.09	64.82	64.96	<u>29.32</u>	<b>68.64</b>	52.23	<b>65.33</b>	<b>58.48</b>	<b>58.13</b>
Five-shot	GPT-4o	<u>89.23</u>	<b>68.51</b>	52.29	<u>70.39</u>	<b>42.59</b>	5.36	49.93	<b>64.89</b>	<u>55.40</u>	39.93
	GPT-4o-mini	65.21	<u>52.48</u>	<u>78.40</u>	62.87	29.18	<u>5.40</u>	<u>52.20</u>	55.93	50.21	23.47
	LLaVA-ov-7b	68.66	48.17	<b>80.00</b>	<b>71.27</b>	24.88	4.56	50.45	61.77	51.22	<u>50.43</u>
	LLaVA-ov-72b	82.41	53.16	72.59	0.00	29.58	3.04	48.76	<u>63.57</u>	44.14	23.26
	Qwen2-vl-7b	73.90	51.83	47.71	26.06	28.94	3.69	50.17	47.85	41.27	26.13
	Qwen2-vl-72b	<b>89.75</b>	51.83	57.95	33.71	<u>32.14</u>	4.22	<b>52.85</b>	57.06	47.44	28.59
	Gemini-1.5-flash	73.02	48.95	74.64	68.89	29.53	<b>68.34</b>	50.55	63.45	<b>59.67</b>	<b>59.10</b>

Table 1. Accuracy results on the DriveMLLM benchmark. These metrics are calculated based solely on successfully formatted responses. The abbreviations are defined as follows: L/R denotes Left/Right Judgment Accuracy, F/B denotes Front/Behind Judgment Accuracy, RHD represents Relative Horizontal Distance Measurement Accuracy, RD is Relative Distance Measurement Accuracy, PPos indicates Pixel Position Localization Accuracy, BBox is Bounding Box Localization Accuracy, CVD represents Camera Vertical Distance Measurement Accuracy, CD is Camera Distance Measurement Accuracy, and AccS signifies the Aggregate Accuracy Score. The column Score denotes the final score of our benchmark.

By multiplying the individual accuracy  $acc_i$  with the efficiency indicator  $eff_i$  for each sample, we ensure that only correctly formatted and accurate predictions contribute to the final score.

### 4.3. Main Results

The models are assessed on both relative and absolute spatial reasoning tasks. In Table 1, we report the accuracy of each spatial evaluation as well as the aggregate accuracy score (AccS) for each model across different tasks. Gemini-1.5-Flash consistently achieves the highest AccS across all experimental settings, indicating superior spatial reasoning capabilities. Gemini-1.5-Flash attains the best score on all shot evaluations outperforming other models.

However, another important metric is the success rate, in some scenarios, the MLLM will fail to answer the question. The Efficiency Scores (EffS) under different shot settings can be seen in the Table 3. According to the equation mentioned in section 4.2.3, we report the final score of the

benchmark in Table 2. We finally select one-shot setting as our final benchmark result as most of the model reach the highest EffS under this setting. The conclusion remains the same, Gemini-1.5-Flash outperforms other models in spatial understanding ability. This result is reasonable since among all these models, only Gemini officially admits the model is fin-tuned with spatial understanding ability.

### 4.4. Discussion

**Impact of Few-Shot Learning:** All models exhibit improved performance when provided with one-shot and five-shot examples. The additional context helps models better understand the task requirements, leading to higher AccS and EffS. For example, GPT-4o improves from an AccS of 43.16% in zero-shot to 55.40% in the five-shot setting.

**Model Size and Performance:** Contrary to common observations, we find that performance on spatial tasks does

Model	Relative Position				Absolute Position				Score
	L/R	F/B	RHD	RD	PPos	BBox	CVD	CD	
Random	49.22	45.03	41.03	44.52	25.46	2.05	47.93	48.59	37.98
GPT-4o	<b>90.84</b>	<b>69.37</b>	34.98	9.69	<b>42.39</b>	<u>5.08</u>	0.00	12.99	33.17
GPT-4o-mini	63.41	48.69	6.52	3.37	16.04	3.76	6.65	28.62	22.13
LLaVA-ov-7b	69.44	48.95	<u>78.46</u>	<b>71.34</b>	24.29	4.16	<u>49.77</u>	<u>61.35</u>	<u>50.97</u>
LLaVA-ov-72b	77.46	<u>60.00</u>	44.62	25.29	19.15	1.87	20.34	44.57	36.66
Qwen2-vl-7b	75.72	51.05	<b>80.61</b>	52.76	25.02	2.86	48.93	5.34	42.79
Qwen2-vl-72b	<u>90.31</u>	51.84	1.52	22.57	27.15	3.79	35.28	49.32	35.22
Gemini-1.5-flash	69.90	52.09	64.82	<u>64.28</u>	<u>28.75</u>	<b>68.02</b>	<b>51.87</b>	<b>65.33</b>	<b>58.13</b>

Table 2. Benchmark final scores on each task, which are calculated by efficiency results weighted accuracy results in the one-shot.

not significantly increase as the size of the model is larger. This conclusion differs from existing findings about multi-modal large models. This phenomenon indicates that current SOTA MLLMs still have much room for improvement in spatial understanding. For instance, LLaVA-ov-72b and Qwen2-vl-72b do not outperform LLaVA-ov-7b and Qwen-vl-7b respectively in most tasks under the relative position setting, especially on task RHD and RD.

**Relative vs. Absolute Spatial Reasoning:** Models achieve higher accuracy on relative spatial reasoning tasks compared to absolute ones. This trend indicates that models find it easier to compare positions between objects rather than compute precise spatial measurements. This is also reasonable since most language model pre-training checkpoints, before they were bridged with multi-model ability, are only trained with logic choices not precise number prediction. However, this problem may be solved if future more spatial datasets are used for fine-tuning the MLLMs.

**Formatting Compliance:** Efficiency Scores (EffS) vary significantly among models. Models like Gemini-1.5-Flash maintain high EffS across all tasks, indicating consistent compliance with the output format. Limited to space, please refer to Table 3 for the result.

**Number of Shots:** The ablation study confirms that increasing the number of examples in the prompt enhances model performance up to a point. While there is a notable improvement from zero-shot to one-shot, the gains diminish beyond five-shot, suggesting diminishing returns with additional examples.

**Model-Specific Behavior:** Different models respond differently to the number of shots. For example, LLaVA-ov-7b shows significant improvement from zero-shot to five-shot settings, whereas qwen2-vl-72b exhibits inconsistent performance across shots. This variability indicates that some

models are more capable of leveraging few-shot learning than others.

## 5. Conclusion and Limitation Discussion

In this paper, we collect data from the nuScence dataset and create the first benchmark dataset containing 8 aspects of questions to evaluate the spatial understanding ability under the autonomous driving scenario. The results highlight the current capabilities and limitations of MLLMs in spatial reasoning within autonomous driving contexts. Although models like Gemini-1.5-Flash show promising performance, there is still a gap in achieving human-level understanding, especially in absolute spatial tasks. The limitation of this work remains clear, this work only proposed the DriveMLLM benchmark but hasn’t proposed a clear method to improve the spatial capacity of MLLMs. Future work should explore advanced training techniques and incorporate domain-specific knowledge to enhance spatial comprehension in MLLMs.

**Acknowledgements.** This work was supported by the National Natural Science Foundation of China under Grant 62373356 and the Open Projects Program of the State Key Laboratory of Multimodal Artificial Intelligence Systems.

## References

- [1] Jean-Baptiste Alayrac, Jeff Donahue, Pauline Luc, Antoine Miech, Iain Barr, Yana Hasson, Karel Lenc, Arthur Mensch, Katherine Millican, Malcolm Reynolds, et al. Flamingo: a visual language model for few-shot learning. *Advances in Neural Information Processing Systems*, 35:23716–23736, 2022. 2
- [2] Dosovitskiy Alexey. An image is worth 16x16 words: Transformers for image recognition at scale. *arXiv preprint arXiv: 2010.11929*, 2020. 2
- [3] Stanislaw Antol, Aishwarya Agrawal, Jiasen Lu, Margaret Mitchell, Dhruv Batra, C Lawrence Zitnick, and Devi Parikh. Vqa: Visual question answering. In *Proceedings of the IEEE international conference on computer vision*, pages 2425–2433, 2015. 2



- [4] Jinze Bai, Shuai Bai, Yunfei Chu, Zeyu Cui, Kai Dang, Xiaodong Deng, Yang Fan, Wenbin Ge, Yu Han, Fei Huang, et al. Qwen technical report. *arXiv preprint arXiv:2309.16609*, 2023. 2
- [5] Jinze Bai, Shuai Bai, Shusheng Yang, Shijie Wang, Sinan Tan, Peng Wang, Junyang Lin, Chang Zhou, and Jingren Zhou. Qwen-vl: A versatile vision-language model for understanding, localization, text reading, and beyond, 2023. 2
- [6] Jinze Bai, Shuai Bai, Shusheng Yang, Shijie Wang, Sinan Tan, Peng Wang, Junyang Lin, Chang Zhou, and Jingren Zhou. Qwen-vl: A versatile vision-language model for understanding, localization, text reading, and beyond. *arXiv preprint arXiv:2309.12966*, 2023. 2
- [7] Jinze Bai, Shuai Bai, Shusheng Yang, Shijie Wang, Sinan Tan, Peng Wang, Junyang Lin, Chang Zhou, and Jingren Zhou. Qwen-vl: A versatile vision-language model for understanding, localization, text reading, and beyond. *arXiv preprint arXiv:2308.12966*, 2023. 2
- [8] Mayank Bansal, Alex Krizhevsky, and Abhijit Ogale. Chauffeurnet: Learning to drive by imitating the best and synthesizing the worst. *arXiv preprint arXiv:1812.03079*, 2018. 1
- [9] Istvan Barabas, Adrian Todoruț, N Cordoș, and Andreia Molea. Current challenges in autonomous driving. In *IOP conference series: materials science and engineering*, 2017. 1
- [10] Tom Brown, Benjamin Mann, Nick Ryder, Melanie Subbiah, Jared D Kaplan, Prafulla Dhariwal, Arvind Neelakantan, Pranav Shyam, Girish Sastry, Amanda Askell, et al. Language models are few-shot learners. *Advances in neural information processing systems*, 33:1877–1901, 2020. 2
- [11] Holger Caesar, Varun Bankiti, Alex H. Lang, Sourabh Vora, Venice Erin Liong, Qiang Xu, Anush Krishnan, Yu Pan, Giancarlo Baldan, and Oscar Beijbom. nuscenes: A multimodal dataset for autonomous driving. *arXiv preprint arXiv:1903.11027*, 2019. 2, 3, 4
- [12] Soravit Changpinyo, Piyush Sharma, Nan Ding, and Radu Soricut. Conceptual 12M: Pushing web-scale image-text pre-training to recognize long-tail visual concepts. In *CVPR*, 2021. 2
- [13] Soravit Changpinyo, Piyush Sharma, Nan Ding, and Radu Soricut. Conceptual 12m: Pushing web-scale image-text pre-training to recognize long-tail visual concepts. In *CVPR*, pages 3558–3568, 2021. 2
- [14] Jiacheng Chen, Tianhao Liang, Sherman Siu, Zhengqing Wang, Kai Wang, Yubo Wang, Yuansheng Ni, Wang Zhu, Ziyang Jiang, Bohan Lyu, Dongfu Jiang, Xuan He, Yuan Liu, Hexiang Hu, Xiang Yue, and Wenhui Chen. Mega-bench: Scaling multimodal evaluation to over 500 real-world tasks. *arXiv preprint arXiv:2410.10563*, 2024. 3
- [15] Lin Chen, Jisong Li, Xiaoyi Dong, Pan Zhang, Conghui He, Jiaqi Wang, Feng Zhao, and Dahua Lin. Sharegpt4v: Improving large multi-modal models with better captions. *arXiv preprint arXiv:2311.12793*, 2023. 2
- [16] Xi Chen, Josip Djolonga, Piotr Padlewski, Basil Mustafa, Soravit Changpinyo, Jialin Wu, Carlos Riquelme Ruiz, Sebastian Goodman, Xiao Wang, Yi Tay, Siamak Shakeri, Mostafa Dehghani, Daniel Salz, Mario Lucic, Michael Tschannen, Arsha Nagrani, Hexiang Hu, Mandar Joshi, Bo Pang, Ceslee Montgomery, Paulina Pietrzyk, Marvin Ritter, AJ Piergiovanni, Matthias Minderer, Filip Pavetic, Austin Waters, Gang Li, Ibrahim Alabdulmohsin, Lucas Beyer, Julien Amelot, Kenton Lee, Andreas Peter Steiner, Yang Li, Daniel Keysers, Anurag Arnab, Yuanzhong Xu, Keran Rong, Alexander Kolesnikov, Mojtaba Seyedhosseini, Anelia Angelova, Xiaohua Zhai, Neil Houlsby, and Radu Soricut. Pali-x: On scaling up a multilingual vision and language model, 2023. 2
- [17] Yuhua Chen, Wen Li, and Luc Van Gool. ROAD: Reality Oriented Adaptation for Semantic Segmentation of Urban Scenes. *IEEE/CVF Conference on Computer Vision and Pattern Recognition*, 2018. 1
- [18] Zhe Chen, Jiannan Wu, Wenhai Wang, Weijie Su, Guo Chen, Sen Xing, Muyan Zhong, Qinglong Zhang, Xizhou Zhu, Lewei Lu, et al. Internvl: Scaling up vision foundation models and aligning for generic visual-linguistic tasks. In *CVPR*, pages 24185–24198, 2024. 2
- [19] Qing Cheng, Niclas Zeller, and Daniel Cremers. Vision-based large-scale 3d semantic mapping for autonomous driving applications. In *International Conference on Robotics and Automation (ICRA)*, pages 9235–9242, 2022. 1
- [20] Marius Cordts, Mohamed Omran, Sebastian Ramos, Timo Rehfeld, Markus Enzweiler, Rodrigo Benenson, Uwe Franke, Stefan Roth, and Bernt Schiele. The Cityscapes Dataset for Semantic Urban Scene Understanding. In *Proceedings of the IEEE/CVF Conference on Computer Vision and Pattern Recognition (CVPR)*, 2016. 1
- [21] Wenliang Dai, Junnan Li, Dongxu Li, Anthony Meng Huat Tiong, Junqi Zhao, Weisheng Wang, Boyang Li, Pascale Fung, and Steven Hoi. Instructblip: Towards general-purpose vision-language models with instruction tuning, 2023. 2
- [22] Qiaole Dong and Yanwei Fu. MemFlow: Optical Flow Estimation and Prediction with Memory. In *Proceedings of the IEEE/CVF Conference on Computer Vision and Pattern Recognition*, 2024. 1
- [23] Xiaoyi Dong, Pan Zhang, Yuhang Zang, Yuhang Cao, Bin Wang, Linke Ouyang, Xilin Wei, Songyang Zhang, Haodong Duan, Maosong Cao, Wenwei Zhang, Yining Li, Hang Yan, Yang Gao, Xinyue Zhang, Wei Li, Jingwen Li, Kai Chen, Conghui He, Xingcheng Zhang, Yu Qiao, Dahua Lin, and Jiaqi Wang. Internlm-xcomposer2: Mastering free-form text-image composition and comprehension in vision-language large model. *arXiv preprint arXiv:2401.16420*, 2024. 2
- [24] Andreas Ess, Konrad Schindler, Bastian Leibe, and Luc Van Gool. Object Detection and Tracking for Autonomous Navigation in Dynamic Environments. *International Journal of Robotics Research (IJRR)*, 2010. 1
- [25] Yuxin Fang, Wen Wang, Binhui Xie, Quan Sun, Ledell Wu, Xinggang Wang, Tiejun Huang, Xinlong Wang, and Yue Cao. Eva: Exploring the limits of masked visual representation learning at scale. In *Proceedings of the IEEE/CVF Conference on Computer Vision and Pattern Recognition*, pages 19358–19369, 2023. 2
- [26] Chaoyou Fu, Peixian Chen, Yunhang Shen, Yulei Qin, Mengdan Zhang, Xu Lin, Jinrui Yang, Xiawu Zheng, Ke Li, Xing Sun, et al. Mme: A comprehensive evaluation benchmark for multimodal large language models. *arXiv preprint arXiv:2306.13394*, 2023. 2, 3

- [27] Xingyu Fu, Yushi Hu, Bangzheng Li, Yu Feng, Haoyu Wang, Xudong Lin, Dan Roth, Noah A Smith, Wei-Chiu Ma, and Ranjay Krishna. Blink: Multimodal large language models can see but not perceive. *European Conference on Computer Vision (ECCV)*, 2024. 3
- [28] Xingyu Fu, Ben Zhou, Ishaan Chandratreya, Carl Vondrick, and Dan Roth. There’s a time and place for reasoning beyond the image. In Smaranda Muresan, Preslav Nakov, and Aline Villavicencio, editors, *Proceedings of the 60th Annual Meeting of the Association for Computational Linguistics (Volume 1: Long Papers)*, pages 1138–1149, Dublin, Ireland, May 2022. Association for Computational Linguistics. 2
- [29] Jiyang Gao, Chen Sun, Hang Zhao, Yi Shen, Dragomir Anguelov, Congcong Li, and Cordelia Schmid. Vectornet: Encoding hd maps and agent dynamics from vectorized representation. In *Proceedings of the IEEE/CVF Conference on Computer Vision and Pattern Recognition (CVPR)*, June 2020. 1
- [30] Andreas Geiger, Philip Lenz, Christoph Stiller, and Raquel Urtasun. Vision meets robotics: The kitti dataset. *The International Journal of Robotics Research*, 32(11):1231–1237, 2013. 1
- [31] Yash Goyal, Tejas Khot, Douglas Summers-Stay, Dhruv Batra, and Devi Parikh. Making the V in VQA matter: Elevating the role of image understanding in Visual Question Answering. In *Conference on Computer Vision and Pattern Recognition (CVPR)*, 2017. 2
- [32] Junru Gu, Chen Sun, and Hang Zhao. Densetnt: End-to-end trajectory prediction from dense goal sets. In *Proceedings of the IEEE/CVF International Conference on Computer Vision*, pages 15303–15312, 2021. 1
- [33] Tianrui Guan, Fuxiao Liu, Xiyang Wu, Ruiqi Xian, Zongxia Li, Xiaoyu Liu, Xijun Wang, Lichang Chen, Furong Huang, Yaser Yacoob, Dinesh Manocha, and Tianyi Zhou. Hallusionbench: An advanced diagnostic suite for entangled language hallucination & visual illusion in large vision-language models, 2023. 3
- [34] Yuhang He, Shi Chen, Yifeng Pan, and Kai Ni. Using Edit Distance and Junction Feature to Detect and Recognize Arrow Road Marking. In *International Conference on Intelligent Transportation Systems (ITSC)*, 2014. 1
- [35] Yuhang He, Ziyu Pan, Lingxi Li, Yunxiao Shan, Dongpu Cao, and Long Chen. Real-Time Vehicle Detection from Short-range Aerial Image with Compressed MobileNet. In *International Conference on Robotics and Automation (ICRA)*, 2019. 1
- [36] Congrui Hetang, Haoru Xue, Cindy Le, Tianwei Yue, Wenping Wang, and Yihui He. Segment Anything Model for Road Network Graph Extraction. In *Proceedings of the IEEE/CVF Conference on Computer Vision and Pattern Recognition (CVPR) Workshops*, 2024. 1
- [37] Yushi\* Hu, Hang\* Hua, Zhengyuan Yang, Weijia Shi, Noah A Smith, and Jiebo Luo. Promptcap: Prompt-guided task-aware image captioning. *arXiv preprint arXiv:2211.09699*, 2022. 2
- [38] Wei-Chih Hung, Henrik Kretzschmar, Tsung-Yi Lin, Yuning Chai, Ruichi Yu, Ming-Hsuan Yang, and Dragomir Anguelov. Soda: Multi-object tracking with soft data association. *arXiv 2008.07725*, 2020. 1
- [39] Ranjay Krishna, Yuke Zhu, Oliver Groth, Justin Johnson, Kenji Hata, Joshua Kravitz, Stephanie Chen, Yannis Kalantidis, Li-Jia Li, David A Shamma, et al. Visual genome: Connecting language and vision using crowdsourced dense image annotations. *International journal of computer vision*, 123:32–73, 2017. 2
- [40] Ranjay Krishna, Yuke Zhu, Oliver Groth, Justin Johnson, Joshua Kravitz, Stephanie Chen, Yannis Kalantidis, Li-Jia Li, David A. Shamma, Michael S. Bernstein, and Fei-Fei Li. Visual Genome: Connecting Language and Vision Using Crowdsourced Dense Image Annotations. In *International Journal of Computer Vision (IJCV)*, 2017. 1
- [41] Bohao Li, Yuying Ge, Yixiao Ge, Guangzhi Wang, Rui Wang, Ruimao Zhang, and Ying Shan. Seed-bench-2: Benchmarking multimodal large language models. *arXiv preprint arXiv:2311.17092*, 2023. 2, 3
- [42] Bohao Li, Rui Wang, Guangzhi Wang, Yuying Ge, Yixiao Ge, and Ying Shan. Seed-bench: Benchmarking multimodal llms with generative comprehension. *arXiv preprint arXiv:2307.16125*, 2023. 2, 3
- [43] Junnan Li, Dongxu Li, Silvio Savarese, and Steven Hoi. Blip-2: Bootstrapping language-image pre-training with frozen image encoders and large language models. *arXiv preprint arXiv:2301.12597*, 2023. 2
- [44] Junnan Li, Dongxu Li, Silvio Savarese, and Steven Hoi. Blip-2: Bootstrapping language-image pre-training with frozen image encoders and large language models, 2023. 2
- [45] Zenan Li, Fan Nie, Qiao Sun, Fang Da, and Hang Zhao. Uncertainty-aware decision transformer for stochastic driving environments. *arXiv preprint arXiv:2309.16397*, 2023. 1
- [46] Tsung-Yi Lin, Michael Maire, Serge Belongie, James Hays, Pietro Perona, Deva Ramanan, Piotr Dollár, and C Lawrence Zitnick. Microsoft coco: Common objects in context. In *Computer Vision—ECCV 2014: 13th European Conference, Zurich, Switzerland, September 6-12, 2014, Proceedings, Part V 13*, pages 740–755. Springer, 2014. 2
- [47] Haotian Liu, Chunyuan Li, Yuheng Li, and Yong Jae Lee. Improved baselines with visual instruction tuning, 2023. 2
- [48] Haotian Liu, Chunyuan Li, Yuheng Li, Bo Li, Yuanhan Zhang, Sheng Shen, and Yong Jae Lee. Llava-next: Improved reasoning, ocr, and world knowledge, January 2024. 2
- [49] Haotian Liu, Chunyuan Li, Qingyang Wu, and Yong Jae Lee. Visual instruction tuning. *Advances in neural information processing systems*, 36, 2024. 2
- [50] Yuan Liu, Haodong Duan, Yuanhan Zhang, Bo Li, Songyang Zhang, Wangbo Zhao, Yike Yuan, Jiaqi Wang, Conghui He, Ziwei Liu, Kai Chen, and Dahua Lin. Mmbench: Is your multi-modal model an all-around player?, 2023. 2, 3
- [51] Yuliang Liu, Zhang Li, Biao Yang, Chunyuan Li, Xucheng Yin, Cheng lin Liu, Lianwen Jin, and Xiang Bai. On the hidden mystery of ocr in large multimodal models, 2024. 2
- [52] Yicheng Liu, Jinghuai Zhang, Liangji Fang, Qinhong Jiang, and Bolei Zhou. Multimodal motion prediction with stacked transformers. In *Proceedings of the IEEE/CVF Conference on Computer Vision and Pattern Recognition*, pages 7577–7586, 2021. 1
- [53] Jiasen Lu, Christopher Clark, Sangho Lee, Zichen Zhang,

- Savya Khosla, Ryan Marten, Derek Hoiem, and Aniruddha Kembhavi. Unified-io 2: Scaling autoregressive multimodal models with vision, language, audio, and action. *arXiv preprint arXiv:2312.17172*, 2023. 2
- [54] Pan Lu, Hritik Bansal, Tony Xia, Jiacheng Liu, Chunyuan Li, Hannaneh Hajishirzi, Hao Cheng, Kai-Wei Chang, Michel Galley, and Jianfeng Gao. Mathvista: Evaluating mathematical reasoning of foundation models in visual contexts. *arXiv preprint arXiv:2310.02255*, 2023. 3
- [55] Ao Luo, Xin Li, Fan Yang, Jiangyu Liu, Haoqiang Fan, and Shuaicheng Liu. FlowDiffuser: Advancing Optical Flow Estimation with Diffusion Models. In *Proceedings of the IEEE/CVF Conference on Computer Vision and Pattern Recognition*, 2024. 1
- [56] Will Maddern, Geoff Pascoe, Chris Linegar, and Paul Newman. 1 Year, 1000km: The Oxford RobotCar Dataset. *The International Journal of Robotics Research (IJRR)*, 2017. 1
- [57] Nigamaa Nayakanti, Rami Al-Rfou, Aurick Zhou, Kratarth Goel, Khaled S Refaat, and Benjamin Sapp. Wayformer: Motion forecasting via simple & efficient attention networks. In *2023 IEEE International Conference on Robotics and Automation (ICRA)*, pages 2980–2987. IEEE, 2023. 1
- [58] OpenAI. Gpt-4 technical report, 2023. 1, 2
- [59] OpenAI. Hello gpt-4o, 2024. [Accessed: 2024-05-26]. 2
- [60] Vicente Ordonez, Girish Kulkarni, and Tamara L Berg. Im2text: Describing images using 1 million captioned photographs. In *NeurIPS*, 2011. 2
- [61] Vicente Ordonez, Girish Kulkarni, and Tamara L Berg. Visual instruction tuning. In *NIPS*, 2011. 2
- [62] Dean A Pomerleau. Alvin: An autonomous land vehicle in a neural network. *Advances in neural information processing systems*, 1, 1988. 1
- [63] Alec Radford, Jong Wook Kim, Chris Hallacy, Aditya Ramesh, Gabriel Goh, Sandhini Agarwal, Girish Sastry, Amanda Askell, Pamela Mishkin, Jack Clark, et al. Learning transferable visual models from natural language supervision. In *International conference on machine learning*, pages 8748–8763. PMLR, 2021. 2
- [64] Alec Radford, Jong Wook Kim, Chris Hallacy, Aditya Ramesh, Gabriel Goh, Sandhini Agarwal, Girish Sastry, Amanda Askell, Pamela Mishkin, Jack Clark, et al. Learning transferable visual models from natural language supervision. In *ICML*, pages 8748–8763, 2021. 2
- [65] Mohd Nizam Saad, Zurina Muda, Noraidah Sahari Ashaari, Hamzaini Abdul Hamid, and Nur Hasanah binti Abu Hasan. The Spatial Relation Features for Describing Objects Relationships within Image. In *International Conference on Electrical Engineering and Informatics (ICEEI)*, 2015. 1
- [66] Christoph Schuhmann, Richard Vencu, Romain Beaumont, Robert Kaczmarczyk, Clayton Mullis, Aarush Katta, Theo Coombes, Jenia Jitsev, and Aran Komatsuzaki. Laion-400m: Open dataset of clip-filtered 400 million image-text pairs. *arXiv preprint arXiv:2111.02114*, 2021. 2
- [67] Christoph Schuhmann, Richard Vencu, Romain Beaumont, Robert Kaczmarczyk, Clayton Mullis, Aarush Katta, Theo Coombes, Jenia Jitsev, and Aran Komatsuzaki. Laion-400m: Open dataset of clip-filtered 400 million image-text pairs. *arXiv preprint arXiv:2111.02114*, 2021. 2
- [68] Dustin Schwenk, Apoorv Khandelwal, Christopher Clark, Kenneth Marino, and Roozbeh Mottaghi. A-okvqa: A benchmark for visual question answering using world knowledge. In *European Conference on Computer Vision*, pages 146–162. Springer, 2022. 2
- [69] Quan Sun, Yuxin Fang, Ledell Wu, Xinlong Wang, and Yue Cao. Eva-clip: Improved training techniques for clip at scale. *arXiv preprint arXiv:2303.15389*, 2023. 2
- [70] Gemini Team, Rohan Anil, Sebastian Borgeaud, Yonghui Wu, Jean-Baptiste Alayrac, Jiahui Yu, Radu Soricut, Johan Schalkwyk, Andrew M Dai, Anja Hauth, et al. Gemini: a family of highly capable multimodal models. *arXiv preprint arXiv:2312.11805*, 2023. 1
- [71] Qwen Team. Introducing qwen1.5, February 2024. 2
- [72] Wei Han Wang, Qingsong Lv, Wenmeng Yu, Wenyi Hong, Ji Qi, Yan Wang, Junhui Ji, Zhuoyi Yang, Lei Zhao, Xixuan Song, Jiazheng Xu, Bin Xu, Juanzi Li, Yuxiao Dong, Ming Ding, and Jie Tang. Cogvlm: Visual expert for pretrained language models, 2023. 2
- [73] Xuan Xiong, Yicheng Liu, Tianyuan Yuan, Yue Wang, Yilun Wang, and Zhao Hang. Neural map prior for autonomous driving. In *Proceedings of the IEEE/CVF International Conference on Computer Vision (CVPR)*, 2023. 1
- [74] Weihao Yu, Zhengyuan Yang, Linjie Li, Jianfeng Wang, Kevin Lin, Zicheng Liu, Xinchao Wang, and Lijuan Wang. Mm-vet: Evaluating large multimodal models for integrated capabilities. *arXiv preprint arXiv:2308.02490*, 2023. 2, 3
- [75] Xiang Yue, Yuansheng Ni, Kai Zhang, Tianyu Zheng, Ruoyi Liu, Ge Zhang, Samuel Stevens, Dongfu Jiang, Weiming Ren, Yuxuan Sun, Cong Wei, Botao Yu, Ruibin Yuan, Renliang Sun, Ming Yin, Boyuan Zheng, Zhenzhu Yang, Yibo Liu, Wenhao Huang, Huan Sun, Yu Su, and Wenhua Chen. Mmmu: A massive multi-discipline multimodal understanding and reasoning benchmark for expert agi. *arXiv preprint arXiv:2311.16502*, 2023. 3
- [76] Rowan Zellers, Yonatan Bisk, Ali Farhadi, and Yejin Choi. From recognition to cognition: Visual commonsense reasoning. In *The IEEE Conference on Computer Vision and Pattern Recognition (CVPR)*, June 2019. 2
- [77] Hang Zhao, Jiyang Gao, Tian Lan, Chen Sun, Ben Sapp, Balakrishnan Varadarajan, Yue Shen, Yi Shen, Yuning Chai, Cordelia Schmid, Congcong Li, and Dragomir Anguelov. Tnt: Target-driven trajectory prediction. In Jens Kober, Fabio Ramos, and Claire Tomlin, editors, *Proceedings of the 2020 Conference on Robot Learning*, volume 155 of *Proceedings of Machine Learning Research*, pages 895–904. PMLR, 16–18 Nov 2021. 1
- [78] Deyao Zhu, Jun Chen, Xiaoqian Shen, Xiang Li, and Mohamed Elhoseiny. Minigpt-4: Enhancing vision-language understanding with advanced large language models. *arXiv preprint arXiv:2304.10592*, 2023. 2

N-shot	Model	Relative Position				Absolute Position				EffS	Score
		L/R	F/B	RHD	RD	PPos	BBox	CVD	CD		
-	Random	100.00	100.00	100.00	100.00	100.00	100.00	100.00	100.00	100.00	37.98
Zero-shot	GPT-4o	<u>91.62</u>	99.48	72.77	7.33	<u>99.89</u>	<u>99.66</u>	1.25	0.34	59.04	<u>25.63</u>
	GPT-4o-mini	90.31	<u>99.74</u>	1.57	0.00	59.66	88.18	0.00	0.80	42.53	16.68
	LLaVA-ov-7b	81.41	<b>100.00</b>	69.11	0.00	<b>100.00</b>	<b>100.00</b>	0.00	0.00	56.32	22.29
	LLaVA-ov-72b	<b>98.69</b>	<b>100.00</b>	18.32	<u>26.18</u>	<b>100.00</b>	<b>100.00</b>	0.34	<u>14.77</u>	57.29	21.10
	Qwen2-vl-7b	84.29	<u>99.74</u>	<u>99.48</u>	3.66	91.70	97.84	<u>30.80</u>	0.68	<u>63.52</u>	21.17
	Qwen2-vl-72b	86.65	<b>100.00</b>	0.00	0.00	<b>100.00</b>	99.32	0.00	0.00	48.25	20.11
	Gemini-1.5-flash	81.41	<b>100.00</b>	<b>100.00</b>	<b>100.00</b>	98.18	97.73	<b>98.64</b>	<b>99.77</b>	<b>96.97</b>	<b>54.03</b>
One-shot	GPT-4o	<u>99.74</u>	<b>100.00</b>	<u>95.81</u>	13.61	<u>99.89</u>	<u>99.55</u>	17.05	20.34	68.25	33.17
	GPT-4o-mini	96.07	<u>99.48</u>	7.85	5.76	62.39	94.66	12.61	51.82	53.83	22.13
	LLaVA-ov-7b	97.38	<b>100.00</b>	<b>100.00</b>	<b>100.00</b>	<b>100.00</b>	<b>100.00</b>	<b>99.77</b>	<u>99.09</u>	<b>99.53</b>	<u>50.97</u>
	LLaVA-ov-72b	97.91	95.29	90.58	37.17	67.05	84.77	38.30	73.18	73.03	36.66
	Qwen2-vl-7b	97.91	<b>100.00</b>	<b>100.00</b>	72.25	98.30	99.32	98.30	10.00	84.51	42.79
	Qwen2-vl-72b	<b>100.00</b>	<b>100.00</b>	3.14	29.84	<b>100.00</b>	98.30	71.36	81.02	72.96	35.22
	Gemini-1.5-flash	99.21	<b>100.00</b>	<b>100.00</b>	<u>98.95</u>	98.07	99.09	<u>99.32</u>	<b>100.00</b>	<u>99.33</u>	<b>58.13</b>
Five-shot	GPT-4o	<b>99.74</b>	<u>99.74</u>	<u>98.43</u>	23.56	99.55	<u>98.52</u>	27.73	50.11	74.67	39.93
	GPT-4o-mini	91.10	<u>99.74</u>	9.42	13.61	67.27	<u>96.59</u>	12.73	<u>51.14</u>	55.20	23.47
	LLaVA-ov-7b	90.84	<b>100.00</b>	<b>100.00</b>	<b>100.00</b>	<u>99.77</u>	<b>100.00</b>	<b>100.00</b>	<b>100.00</b>	<u>98.83</u>	<u>50.43</u>
	LLaVA-ov-72b	<b>99.74</b>	99.48	25.13	0.00	96.93	89.66	1.70	0.91	51.69	23.26
	Qwen2-vl-7b	90.58	<b>100.00</b>	10.99	3.14	93.52	<b>100.00</b>	97.61	9.32	63.15	26.13
	Qwen2-vl-72b	<b>99.74</b>	<b>100.00</b>	1.57	<u>28.80</u>	<b>100.00</b>	97.95	72.73	3.64	63.05	28.59
	Gemini-1.5-flash	<u>96.86</u>	<b>100.00</b>	<b>100.00</b>	<b>100.00</b>	97.50	98.18	<u>99.43</u>	<b>100.00</b>	<b>99.00</b>	<b>59.10</b>

Table 3. Efficiency score on different sub-tasks during the evaluation of the DriveMLLM benchmark.

## Appendix

### A. Efficiency Score

When prompting the MLLMs to answer the designed spatial questions within an autonomous driving scenario, we observe that not all questions are successfully addressed by the models. This failure arises either because the MLLMs do not adhere to the instructed response format or because they decline to provide an answer due to uncertainty. To evaluate the models’ compliance with the required output format—which is crucial for automated assessment—we utilize the Efficiency metrics defined in the main paper. For each sample  $i$ , we define the efficiency indicator  $\text{eff}_i$  as:

$$\text{eff}_i = \begin{cases} 1, & \text{correctly formatted} \\ 0, & \text{otherwise} \end{cases} \quad (9)$$

The Efficiency Score (EffS) is calculated as:

$$\text{eff} = \frac{1}{N} \sum_{i=1}^N \text{eff}_i \quad \text{EffS} = \frac{1}{8} \sum_{j=1}^8 \text{eff}_j \quad (10)$$

The results are presented in Table 3. It is observed that the Gemini-1.5-flash model outperforms the other models in most scenarios, which aligns with the comparison results in the accuracy evaluation. Furthermore, most models achieve their highest performance under the one-shot setting. This observation led us to adopt the one-shot setting for the final benchmark results, as discussed in the main paper.